Progress In Electromagnetics Research C, Vol. 125, 93–104, 2022

A Nested Slot and T-Match Network Based Hybrid Antenna for UHF RFID Tag Applications

Amit K. Singh[1, *], Sudhir Bhaskar[2], and Amit K. Singh[1]

Abstract—A planar UHF RFID tag antenna with a hybrid nested slot and T-match network is presented. A novel T-match network in a nested slot is introduced to have superior conjugate impedance matching between tag antenna and the semiconductor microchip. Size curtailment is acquired by means of exploiting the T-match network branches and feeder strip line. Moreover, expanding the nested slot area and increasing the T-match branch length modify the electrical length and increase the antenna inductance. Thus by utilizing the arm of matching network and feeder, conjugate impedance is achieved in accordance with the semiconductor chip at 865 MHz. A surpassing UHF tag with volume $120 \times 60 \times 1.6\,\text{mm}^3$ ($0.346\lambda \times 0.173\lambda \times 0.0046\lambda$), with outstanding 10-dB return loss of 12 MHz, has been flourishingly demonstrated, and it is able to obtain a detection range of 13.9 m. This tag antenna composition is simulated with respect to 4 W EIRP reader.

1. INTRODUCTION

In recent past years, Radio Frequency Identification (RFID) technique has been reaching its heights in the area of Agriculture, EPS (Electronic Payment Systems), Access control, Libraries, Marathons, Hospitals, and many more resourceful applications [1, 2]. RFID systems work on Low frequency (125–134) kHz, HF (13.56 MHz), UHF band (433 MHz and 840 to 960 MHz), and microwave frequency band (2.45 and 5.8 GHz) [3]. A particular country or region has allocated specific frequency band [4]. Some of the region-wise allocated frequency bands are shown in Table 1.

RFID tags in UHF band are most needed in today's commercial world. UHF RFID tags are smaller in size than LF and HF tags along with less multipath interference. They provide higher read range albeit low transmitting power. In UHF RFID tag, backscatter modulation technique is used, in which the reader antenna sends EM wave as interrogator to the tag. The UHF tag happens to be nothing but a transducer which converts this incoming interrogator into electrical signal. The UHF tag comprises a semiconductor microchip namely ASIC (Application Specific Integrated Circuit), which is used for input impedance matching [5]. The input impedance of RFID microchip is capacitive in nature, and impedance matching is done with inductive impedance of the UHF tag antenna. Impedance matching techniques in UHF RFID tag design and miniaturization of size were explained in [6]. The complex conjugate impedance matching in UHF RFID tag is actualized by conjoining either of T-match network, inductively coupled loop or nested slot. In T-match method, the input impedance of the dipole is altered by using short circuit stubs. T-match network summates inductive element to the antenna input impedance so that it is able to compensate the capacitive impedance of the microchip.

Matching in T-match network is acquired by altering the length and width of the branches. [7] describes how a T-match tag antenna matches with NXP UCODE G2X IC having impedance $24 - j163\ \Omega$ at 875 MHz. In [8], a T-match network is introduced in the form of loop to match an

Received 14 August 2022, Accepted 3 October 2022, Scheduled 6 October 2022

* Corresponding author: Amit Kumar Singh (amit.kumarsingh.rs.ece18@iitbhu.ac.in).

[1] Electronics Engineering Department, Indian Institute of Technology (BHU), Varanasi, India. [2] Electronics and Communication Engineering, Central University of Rajasthan, Ajmer, India.

Table 1. Region-wise UHF band frequency allocation.

Region	Frequency (MHz)	Power	Region	Frequency (MHz)	Power
America	902–928	4 W EIRP	Jordan	865–868	2 W ERP
China	920.5–924.5	2 W ERP	Russia	866–867.6 866–868 866–867.6 915–921	100 mW ERP 500 mW ERP 2 W ERP 1 W ERP
Denmark	865.6–867.6 916.1–918.9	2 W ERP 4 W ERP	Singapore	866–869 920–925	0.5 W ERP 2 W ERP
Hong Kong	865–868 920–925	2 W ERP 4 W EIRP	South Africa	865.6–867.6 915.4–921	2 W ERP 4 W EIRP
India	865–867	4W ERP	Vietnam	866–868 918–923 920–923	0.5 W ERP 0.5 W ERP 2 W ERP

SRR (Split-Ring Resonator) UHF tag antenna. [9] demonstrates a T-match network for impedance matching with NXP UCODE G2XM microchip with its equivalent circuit analysis and reports a peak read range value of 11 meters at 898 MHz.

Nesting configurations in antenna design for RFID tag have been developing as a prominent contender. This configuration provides multibands, extensive bandwidth [10], complex impedance matching [11] characteristics along with contraction of antenna size [12]. Nested slot based impedance matching is applicable to larger planar dipoles having higher permittivity substrate. In this method, the total slot size is comparable to the patch area. A nested slot configuration in RFID tag used for remote healthcare operations is introduced in [13]. The article matches the tag with impedance of Impinj R6 microchip, although by using a nested slot in patch, mediocre impedance matching was obtained. The maximum read range of the antenna obtained was only 3 meters although the tag had very small size.

It is realized from above literature that impedance matching with microchip is a foremost task for RFID tag design. For this purpose, in previous literatures, three methods, i.e., T-match, Inductive coupled loop, and nested slot, have been used. In this proposed work, a combination of three techniques, i.e., meandered line, T-match, and nested slot, is used to get commendable complex conjugate impedance matching. Thus, the hybridization of aforementioned techniques produces a novel RFID tag antenna in UHF India band. It is realized that this designed antenna has adequate measured read range in contrast with earlier designs. The tag complex impedance, impedance matching with IC Alien Higgs-4 SOT, reflection coefficient, and read range are presented.

2. UHF TAG DESIGN

The geometric schematic of the tendered antenna for UHF RFID tag is shown in Figure 1. The tag has the dimension of 120 mm × 60 mm × 1.6 mm built on a Rogers RT/duroid 5880 substrate ($\epsilon_r = 2.2$, $\tan\delta = 0.0009$) having thickness of 1.6 mm. This antenna is designed inside a nested slot. The tag antenna consists of a symmetric T-match network in the nested slot providing conjugate impedance matching with the microchip. The most available microchips namely ASICs have the resistance up to tens while the capacitive reactance is found to be up to hundreds. The semiconductor microchip used in this RFID UHF tag antenna is Alien Higgs-4 SOT [14], which has the sensitivity of −18.5 dBm during the reading mechanism. The microchip has the complex input impedance of $20.5 - j191.2\,\Omega$ at 865 MHz. The result clarifies that the simulated 10 dB-return loss bandwidth obtained from the proposed tag antenna is 12 MHz (859 MHz–871 MHz).

The resonance frequency is tuned by altering the dimensions of the nested slot, feed line, and

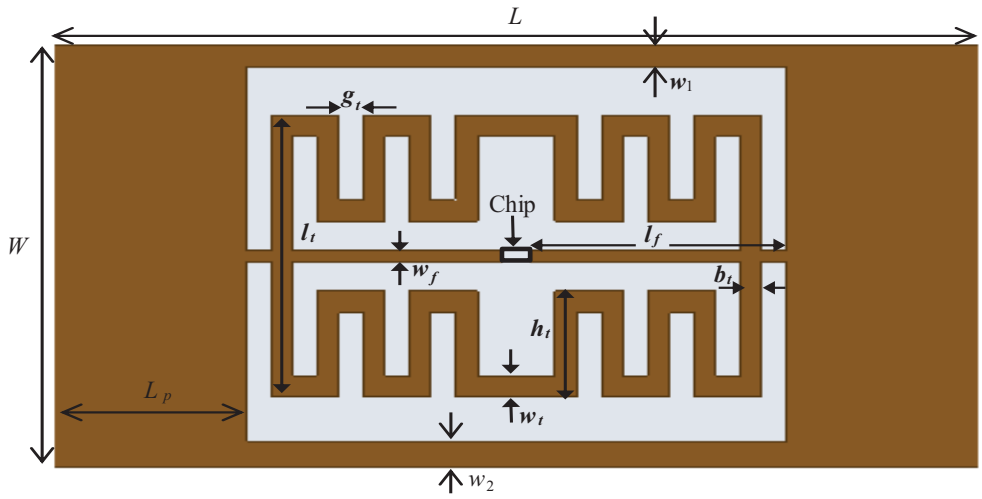

Figure 1. Schematic of the tendered antenna.

introducing T-match, and thus matching the tag impedance with the chip is achieved. The optimum values of geometrical parameters of the proposed antenna to obtain the impedance matching are shown in Table 2. Initially, a nested slot is imposed in the patch, and impedance matching between the antenna and microchip is observed. Due to not perfectly matching with microchip, a T-match network with meander lines is introduced in the nested slot. The steps to achieve the impedance matching with microchip is shown in Figure 2. The overall substrate size ($L \times W$), nested slot area, and the feed length and width remain the same in all steps. The further effects of nested slot, meandered T-match network, and symmetric end structure on various characteristics are now investigated. For the

Table 2. Optimized values of geometrical parameters of the tag antenna.

Parameters	Values (mm)	Parameters	Values (mm)
L	120	b_t	3
W	60	L_p	25
w_t	3	w_f	1.5
l_f	33	w_1	3
g_t	3	w_2	3.5
l_t	40	h_t	15

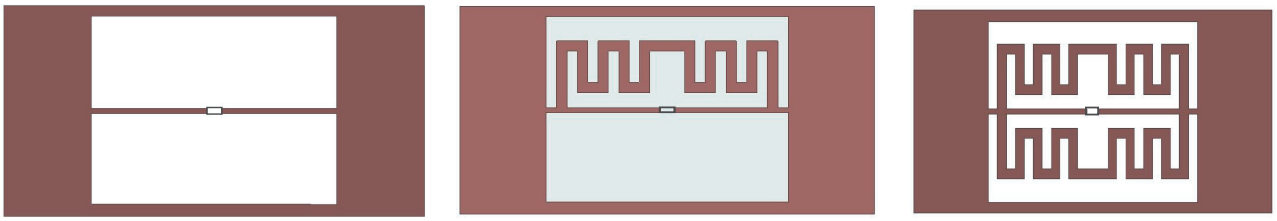

(a) Antenna I (b) Antenna II (c) Antenna III

Figure 2. Transformation steps of proposed antenna. (a) UHF tag with a nested slot. (b) UHF tag with a single-sided T-match network inside a nested slot. (c) UHF tag with a double-sided symmetric T-match network inside a nested slot.

UHF tag antenna design, a nested slot is used for impedance matching as shown in Figure 2(a), and this structure resonates at 845 MHz. In Figure 2(b), the one side nested slot is superimposed by a meandered T-matching network, hence, enabling the tag antenna to resonate at 854 MHz. The inductance of the meandered T-match network can be expressed as [15]:

$$L = 0.2l\left[\ln\left(\frac{l}{w+t}\right) + 1.19 + 0.022\left(\frac{w+t}{l}\right)\right] \text{ nH/mm} \quad (1)$$

where l is the total meandered T-match network length in mm, t the thickness in mm, and w the width in mm. Here, the total length of meandered T-match network, $l = 97$ mm. The thickness (t) and periodic width (w) are 3 mm and 6 mm, respectively.

Figure 2(c) presents the final structure of the tag antenna with a symmetric T-match meandered network inside a nested slot. The symmetric T-match introduces parallel inductance resulting in reduced effective inductance, and the proposed antenna resonates at the desired frequency of 865 MHz. The simulated impedance matching and reflection coefficient of all the three cases are shown in Figure 3.

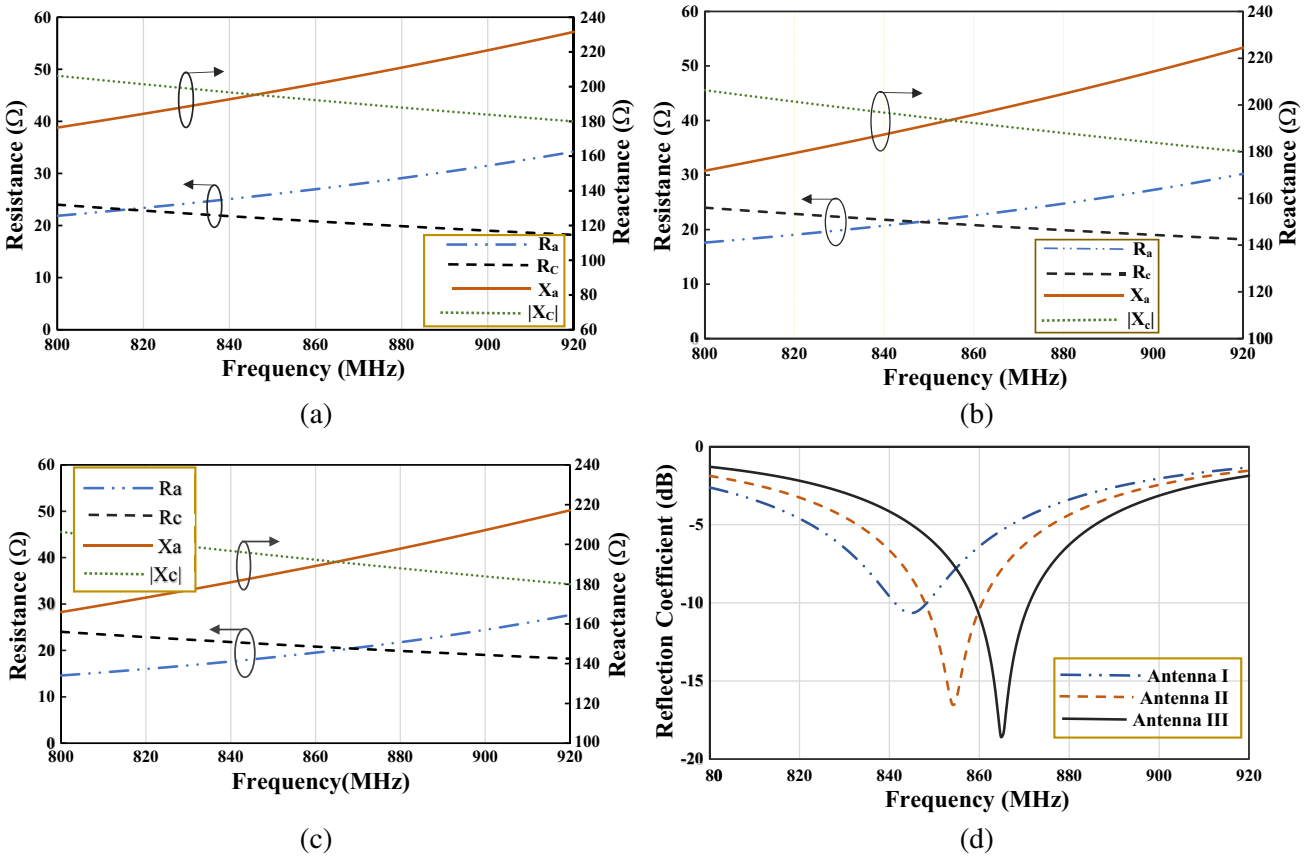

Figure 3. Simulated impedance matching and reflection coefficient of every step. R_a and X_a are resistance and inductive reactance of tag antenna respectively. R_c and $|X_c|$ represents resistance and absolute value of capacitive reactance of microchip respectively. (a) Input impedance of Antenna I. (b) Input impedance of Antenna II. (c) Input impedance of Antenna III. (d) Simulated reflection coefficient.

The first case, i.e., tag antenna with a nested slot, is referred as Antenna I, and its impedance matching graph is shown in Figure 3(a). The second case, i.e., tag antenna with single sided T-match meandered network inside the nested slot, is referred as Antenna II, and its impedance matching graph is shown in Figure 3(b). The final structure, i.e., tag antenna with a double-sided symmetric T-match network inside nested slot, is referred as Antenna III, and its impedance matching graph is shown in Figure 3(c). The simulated reflection coefficient graph of all the three antennas is shown in Figure 3(d).

For the proper functioning of the RFID tag, the tag input impedance should be matched to chip impedance for maximum power transfer. The microchip switches its input impedance in two states, i.e., shorted state & matched state. When the microchip is matched to tag, the incoming signal from reader is absorbed by the transducer, and chip changes to short state. In short state, the interrogator signal is retransmitted to the reader. The obtained impedance of the tag at 865 MHz is $20 + j191.2\,\Omega$. The return loss is calculated by the given formula in Eq. (2):

$$\Gamma = \frac{Z_c - Z_a^*}{Z_c + Z_a} \tag{2}$$

where Z_c and Z_a are microchip and tag input impedances, respectively, where $Z_a = R_a + jX_a$ and $Z_c = R_c + jX_c$, and X_c is negative.

The tag antenna consists of a radiating body and T-match rectangular loop, which are inductively coupled. After combining radiating body and the T-match loop, the two terminals are attached to the microchip. The strength of coupling is controlled by loop-gap, shape of the T-match loop, and the strip width. The equivalent circuit of the rectangular T-matching loop antenna is shown in Figure 4. The tag antenna input impedance is given by [16]

$$Z_a = R_a + jX_a = Z_{Tm} + \frac{(2\pi f M)^2}{Z_r} \tag{3}$$

where Z_r and Z_{TM} are the impedances of radiating body and T-match loop, respectively. M is the mutual inductance between the inductances. Z_r is calculated by:

$$Z_r = R_{r,0} + jR_{r,0}Q_r\left(\frac{f}{f_0} - \frac{f_0}{f}\right) \tag{4a}$$

where $R_{r,0}$ is the resistance of the radiating body at resonance frequency, Q_r the quality factor, and f_0 the resonating frequency. The impedance of T-match network can be calculated by:

$$Z_{Tm} = j2\pi f L_{Tm} \tag{4b}$$

The resistance and reactance at resonating frequency can be calculated by:

$$R_a\,(f = f_0) = \frac{(2\pi f_0 M)^2}{R_{r,0}} \tag{5a}$$

$$X_a\,(f = f_0) = 2\pi f_0 L_{Tm} \tag{5b}$$

where L_{Tm} is the inductance of meandered T-match network which is obtained from Eq. (1). Thus, by using above equations, the real and imaginary parts of the tag antenna impedance is obtained which is plotted in Figure 3(c).

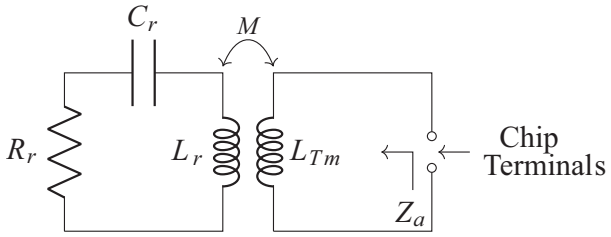

Figure 4. Inductively coupled T-match loop equivalent circuit.

3. PARAMETRIC ANALYSIS

Every geometrical parameter has different effects on input impedance and reflection coefficient of the tendered antenna. Parametric analysis is carried out by altering one parameter at a time and keeping other parameters constant. The impact of variation of meandered T-match network width (w_t), feed line width (w_f), length of T-match network (l_t) on impedance matching and return loss is investigated.

Variation of w_t and l_t shows the effect of T-match network on impedance matching, and w_f indicates the effect of nested slot area on impedance matching.

In order to analyze the response of these parameters on input impedance and return loss, the tag antenna is simulated by varying parameter w_t from 2 mm to 4 mm while keeping other parameters constant. It is realized from Figure 5(a) that the real part of impedance matching increases with the increase in w_t. When w_t is 2 mm, we find that the real part of impedance is matched at 836.7 MHz while imaginary part matches with the semiconductor chip reactance at 854.2 MHz. Thus the difference between resistance matching and reactance matching is 17 MHz, and tag antenna resonates at 853 MHz with poor return loss having 8 MHz 10-dB return loss bandwidth.

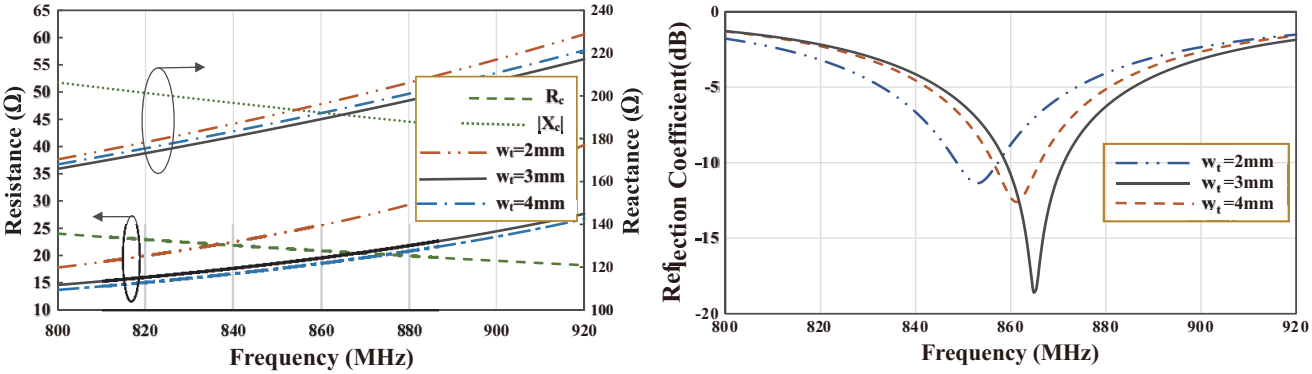

Figure 5. (a) Simulated input impedance and (b) Reflection Coefficient for different values of w_t.

For $w_t = 3$ mm, it is observed that the antenna resonates at 865 MHz with 12 MHz 10-dB return loss bandwidth. When $w_t = 4$ mm, the real part of tag antenna matches with microchip resistance at 875 MHz while reactance matches at 860 MHz. At this value the difference is 15 MHz, and antenna resonates at 861.2 MHz with 9.6 MHz 10-dB return loss bandwidth. The reflection coefficient for these values of w_t is shown in Figure 5(b). Thus, the value of w_t for optimum reflection coefficient is found to be 3 mm.

To investigate the effect of l_t on the performance of tag antenna, it is varied from 38 mm to 42 mm while other parameters are kept constant. From Figure 6, it is realized that we find the optimum return loss for $l_t = 40$ mm.

For $l_t = 38$ mm, the real part of input impedance tag matches with microchip resistance at 881.8 MHz, and imaginary part is matched at 871 MHz. Thus, there is 10.8 MHz frequency gap between

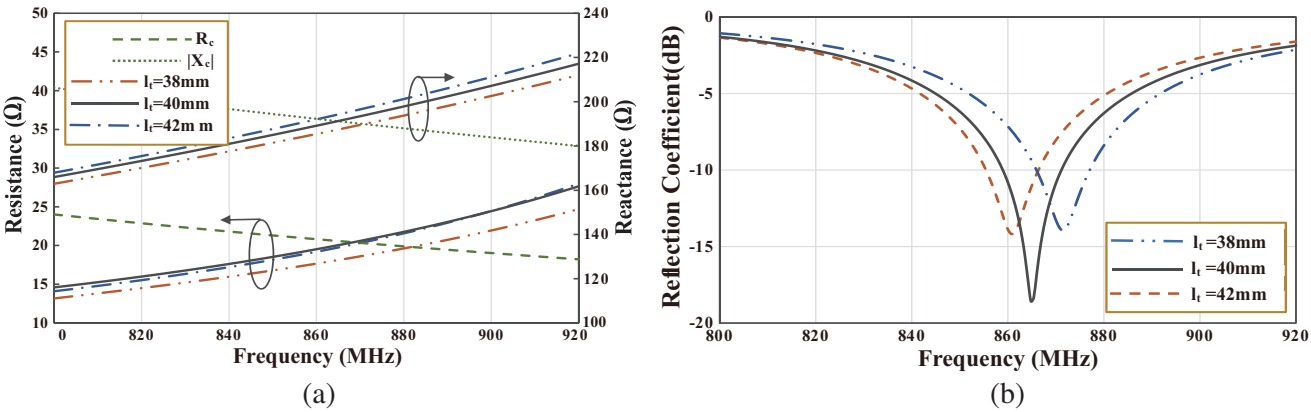

Figure 6. (a) Simulated input Impedance and (b) Reflection Coefficient for different values of l_t.

resistance matching and reactance matching. For this value, tag antenna resonates at 871.4 MHz with 10.8 MHz 10-dB return loss bandwidth. Further, resonating frequency decreases with increasing l_t. For $l_t = 42$ mm, the real part of tag antenna matches with microchip resistance at 870 MHz, and the imaginary part matches with microchip reactance at 860 MHz, thus frequency separation between resistance matching and reactance matching is 10 MHz. Hence tag antenna resonates at 860.6 MHz with poor return loss having 10.2 MHz 10-dB return loss bandwidth.

Figure 7(a) depicts the simulated resistance and reactance of input impedance of the proposed structure with different values of w_f, ranging from 1 mm to 2 mm, keeping other parameters unaltered. For $w_f = 1$ mm, the real parts of tag and microchip impedance are equal at 847 MHz, while the imaginary part matches below the UHF band for RFID tags. Further, increasing the value of w_f, complex impedance matching is achieved at 865 MHz for $w_f = 1.5$ mm. Increasing the value of w_f results in higher resonating frequency. For $w_f = 2$ mm, the real part equals microchip resistance at 872.8 MHz, and imaginary part of tag antenna matches with the reactance of microchip at 886.8 MHz. Thus it is observed that there is a 14 MHz gap. Tag antenna resonates at 885.8 MHz with 10 MHz 10-dB return loss bandwidth. The return losses for these feed line widths are shown in Figure 7(b). It is contemplated from the parametric study that with the optimized values of the aforementioned parameters, the input impedance of UHF tag antenna is $20 + j191.2\,\Omega$ at 865 MHz, which is almost the complex conjugate of the microchip impedance.

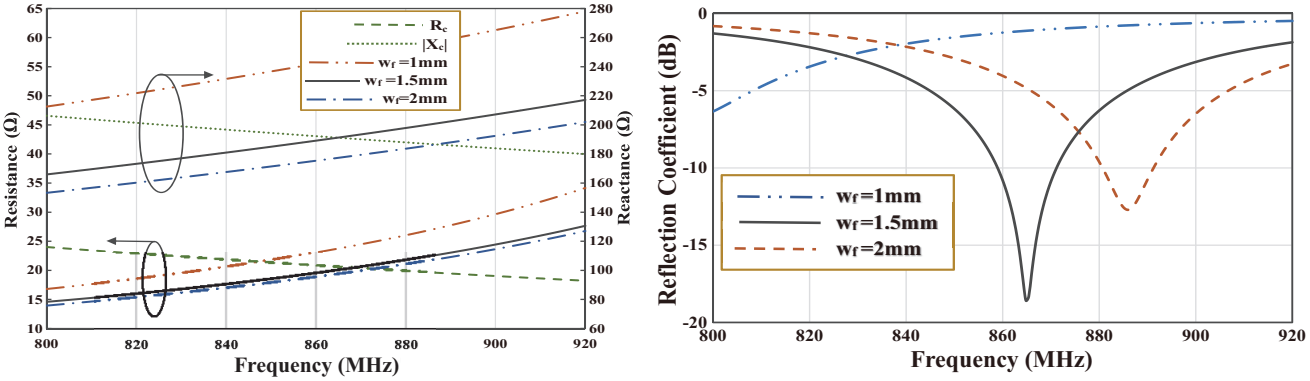

Figure 7. (a) Simulated input impedance and (b) Reflection Coefficient for different values of w_f.

4. RESULTS AND DISCUSSIONS

The fabricated prototype of the RFID tag antenna with a Rogers RT/duroid 5880 substrate is shown in Figure 8. As the proposed antenna structure is a balanced structure, the input impedance and reflection loss cannot be measured by using simply single ended two-port Vector Network Analyser. If a balanced tag antenna is connected to an unbalanced port, then unequal current flows in the tag antenna. Thus accurate measurement of impedance of the balanced tag antenna becomes tough. Hence, authors

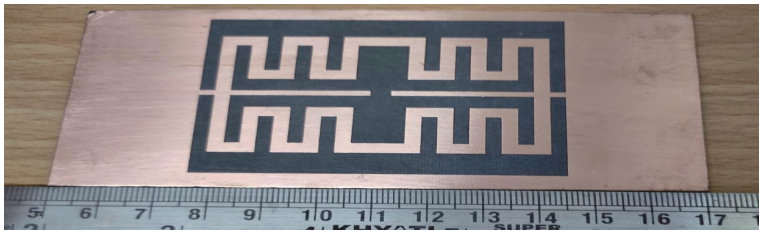

Figure 8. Fabricated prototype of proposed RFID tag antenna.

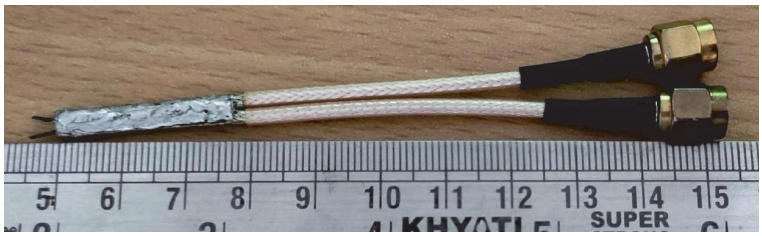

Figure 9. Semi-rigid differential probe used for impedance measurement.

used differential probe method [17] based input impedance measurement which is shown in Figure 9 with Anritsu MS2038C VNA. The measurement setup of impedance using differential probe is shown in Figure 10. One end of the differential probe is connected to the VNA with cables, and the other end, which has small extended inner conductors, is connected to the antenna under test as shown in Figure 11.

The S-parameters of the proposed antenna are measured by aforementioned VNA and then by using following conversion formula [18], the differential input impedance (Z_{diff}) of the tag antenna is

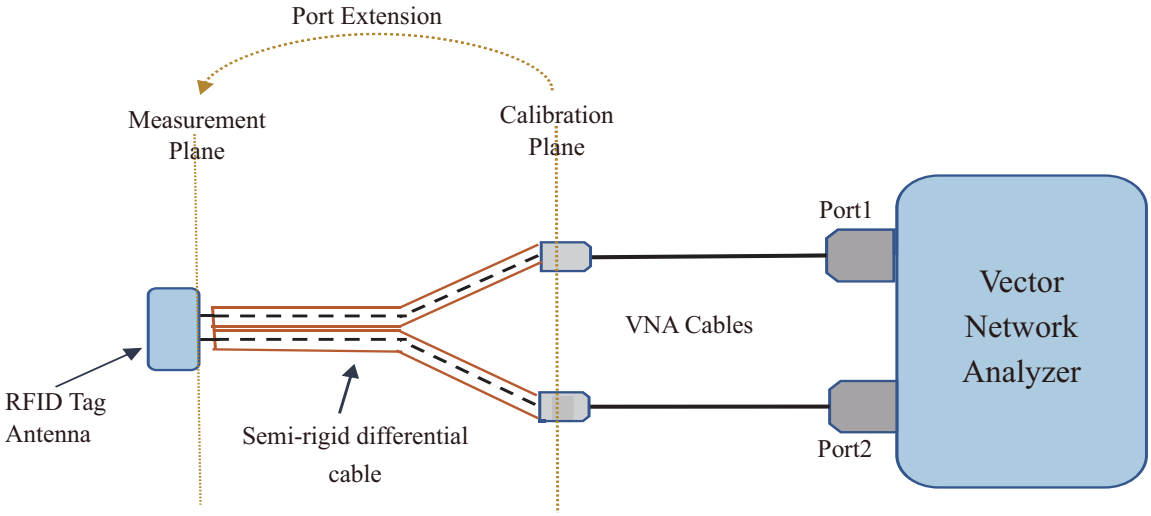

Figure 10. Measurement schematic setup with differential probe.

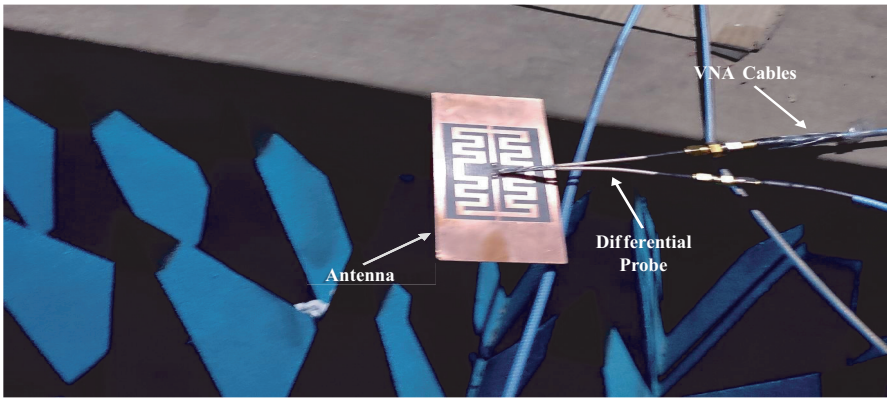

Figure 11. Impedance measurement of tag antenna.

calculated.

$$Z_{diff} = \frac{2Z_0\left(1 - S_{11}S_{22} + S_{12}S_{21} - S_{12} - S_{21}\right)}{\left(1 - S_{11}\right)\left(1 - S_{22}\right) - S_{21}S_{12}} \tag{6}$$

Figures 12 and 13 show measured and simulated input impedances and reflection coefficients of the proposed antenna, respectively. The measured input impedance is $20.9 + j191.2\,\Omega$ at 865 MHz, while the same achieved by simulation is $20 + j191.2\,\Omega$ which is approximate to complex conjugate of microchip impedance. The measured 10-dB reflection coefficient bandwidth is 9 MHz (861.5 MHz–870.5 MHz). The slight incongruity between the measured and simulation results can be attributed to port extension errors and fabrication imperfections.

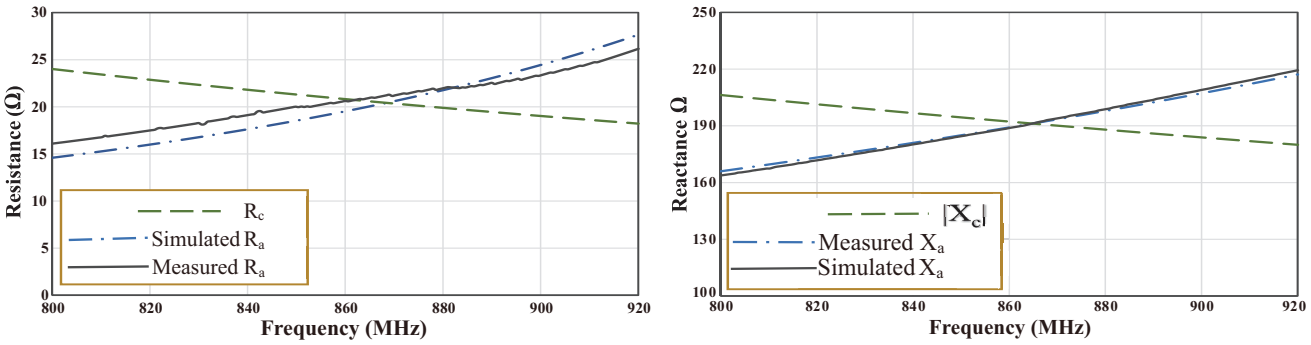

(a) (b)

Figure 12. Measured and simulated input impedance of proposed antenna. (a) Measured and simulated resistance. (b) Measured and simulated reactance.

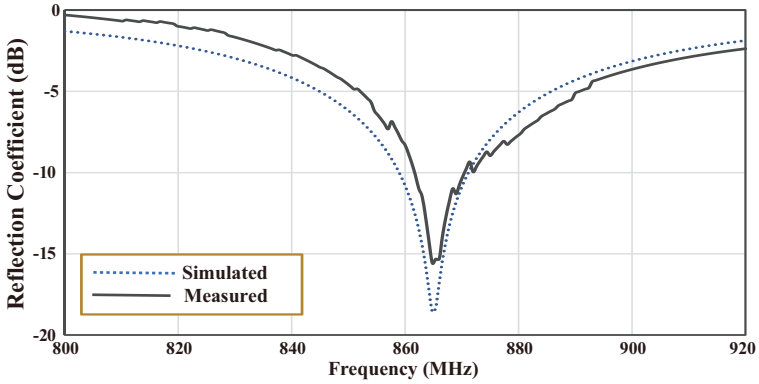

Figure 13. Measured and simulated reflection coefficient of RFID tag antenna.

The maximum separation distance between the reader and tag for activation of chip is given by Eq. (7).

$$S_{\max}(\theta,\phi) = \frac{\lambda}{4\pi}\sqrt{\frac{EIRP_R}{P_{th,chip}}(1 - |\Gamma|^2)G_t(\theta,\phi)} \tag{7}$$

where $G_t(\theta,\phi)$ is the gain of tag antenna, and $(1-|\Gamma|^2)$ is efficiency due to impedance mismatches. The tag is tested for 4 W EIRP reader and the microchip sensitivity, $P_{th,chip} = -18.5$ dBm.

$G_t(\theta,\phi)$ is expressed as [19],

$$G_t(\theta,\phi) = \tau\eta_{cd}D \tag{8}$$

where,

$$\tau = (1 - |\Gamma|^2) \tag{9}$$

is the impedance mismatch efficiency, and η_{cd} is the efficiency as a result of dielectric and conductor losses, i.e., radiation efficiency. The simulated realized gain of every transformation step is shown in Figure 14. Gain of the proposed antenna is over -0.52 dBi covering -10 dB bandwidth. The measured and simulated maximum separations between tag and reader, which is the read range, is sketched in Figure 15.

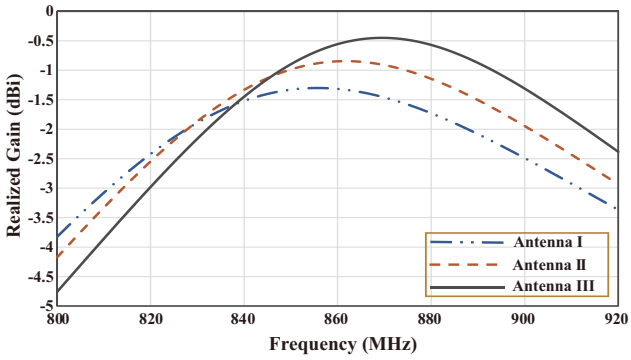

Figure 14. Simulated gain of the tag antenna at the boresight.

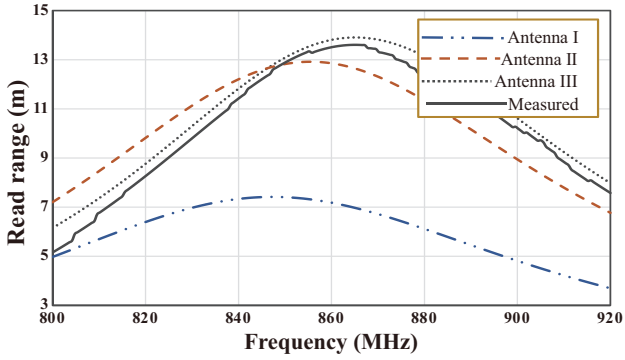

Figure 15. Measured Read range obtained of the proposed tag antenna.

Table 3 testifies a comparison among this work and other erstwhile reported antennas in similar band in terms of chip used, substrate, dimensions, and read range. The comparison is done for those UHF tags which are operated in the same vicinity of frequency of operation as the proposed antenna. The semiconductor microchip used in the proposed work has the lowest sensitivity to provide better tag-reader separation. In the proposed antenna, authors have used a different substrate compared to other works. It can be seen that the achieved gain is much higher than most of the antennas. However, the proposed antenna size has larger dimensions, but it provides far more tag-reader separation distance.

Table 3. Various parameters comparison of the tendered antenna with few previous reported antenna.

Antenna	Microchip	Sensitivity (dBm)	Substrate	Dimensions (mm^3)	Frequency (MHz)	Gain (dBi)	Read range (m)
[20]	Higg-2	-17	FR4	$100 \times 60 \times 10$	870	$--$	12.2
[21]	Higgs-2	-15	FR4	$120 \times 30 \times 1.5$	868	$--$	3.5
[22]	IC of $Z_{in} = 22 - j195\,\Omega$	-15	GML 1000	$105 \times 60 \times 0.76$	866	$--$	7.3
[23]	Monza4	-17.4	RO4350B	$18 \times 4 \times 2$	867	$--$	3
[24]	Higgs-3	-18	FR4	$26 \times 8 \times 1.55$	867	-13	2.8
[25]	Higgs-4	-18.5	Copper-clad alumina	$23 \times 23 \times 1$	866	-17	1.2
[26]	Monza 5	-17.8	PP4 foam	$31.5 \times 31.5 \times 3.2$	867	-5.35	7.25
Proposed work	Higgs-4 SOT	-18.5	RT/duroid 5880 (tm)	$120 \times 60 \times 1.6$	865	-0.47	13.9

5. CONCLUSION

In this article, a novel hybrid T-matched network is produced inside a nested slot. The antenna is matched to Alien Higgs-4 microchip for the maximum power transfer. Parametric analysis of the proposed structure is done. The obtained 10 dB return loss bandwidth is found to be 12 MHz, i.e., RFID tag antenna is operatable in the range of 859 MHz to 871 MHz. The equivalent circuit of the proposed antenna is explained to make it easier to examine the working principle of the tag. As a result, an enhanced separation distance is obtained. This tag antenna spreads its tag to reader separation up to 13.9 meters, which makes it applicable to automatic vehicle identifying applications.

REFERENCES

1. Ruiz-Garcia, L. and L. Lunadei, "The role of RFID in agriculture: Applications, limitations and challenges," *Computers and Electronics in Agriculture*, Vol. 79, No. 1, 42–50, 2011.
2. Domdouzis, K., B. Kumar, and C. Anumba, "Radio-Frequency Identification (RFID) applications: A brief introduction," *Advanced Engineering Informatics*, Vol. 21, No. 4, 350–355, 2007.
3. Bhaskar S., S. Singhal, and A. K. Singh, "Folded-slot active tag antenna for 5.8 GHz RFID applications," *Progress In Electromagnetics Research C*, Vol. 82, 89–97, 2018.
4. Paredes, F., G. Zamora, S. Zuffanelli, F. J. Herraiz-Martinez, F. Martin, and J. Bonache, "Free-space and on-metal dual-band tag for UHF-RFID applications in Europe and USA," *Progress In Electromagnetics Research*, Vol. 141, 577–590, 2013.
5. Barman, B., S. Bhaskar, and A. K. Singh, "Dual-band UHF RFID tag antenna using two eccentric circular rings," *Progress In Electromagnetics Research M*, Vol. 71, 127–136, 2018.
6. Marrocco, G., "The art of UHF RFID antenna design: Impedance-matching and size-reduction techniques," *IEEE Antennas and Propagation Magazine*, Vol. 50, No. 1, 66–79, 2008.
7. Bauernfeind, T., K. Preis, G. Koczka, S. Maier, and O. Biro, "Influence of the non-linear UHF-RFID IC impedance on the backscatter abilities of a T-match tag antenna design," *IEEE Transactions on Magnetics*, Vol. 48, No. 2, 755–758, 2012.
8. Zamora, G., S. Zuffanelli, P. Aguila, F. Paredes, F. Martin, and J. Bonache, "Broadband UHF-RFID passive tag based on Split-Ring Resonator (SRR) and T-match network," *IEEE Antennas and Wireless Propagation Letters*, Vol. 17, No. 3, 517–520, 2018.
9. Zamora, G., S. Zuffanelli, F. Paredes, F. Martı, and J. Bonache, "Design and synthesis methodology for UHF-RFID tags based on the T-match network," *IEEE Transactions on Microwave Theory and Techniques*, Vol. 61, No. 12, 4090–4098, 2013.
10. Sharma, N. and S. S. Bhatia, "Performance enhancement of nested hexagonal ring-shaped compact multiband integrated wideband fractal antennas for wireless applications," *International Journal of RF and Microwave Computer-Aided Engineering*, Vol. 30, No. 3, e22079, 2020.
11. Mark, R., N. Mishra, K. Mandal, P. P. Sarkar, and S. Das, "Hexagonal ring fractal antenna with dumb bell shaped defected ground structure for multiband wireless applications," *AEU —-International Journal of Electronics and Communications*, Vol. 94, 42–50, Sep. 1, 2018.
12. Daniel, R. S., "A CPW-fed rectangular nested loop antenna for penta band wireless applications," *AEU — International Journal of Electronics and Communications*, Vol. 139, 153891, 2021.
13. Sharif, A., J. Ouyang, Y. Yan, A. Raza, M. A. Imran, and Q. H. Abbasi, "Low-cost inkjet-printed RFID tag antenna design for remote healthcare applications," *IEEE Journal of Electromagnetics, RF and Microwaves in Medicine and Biology*, Vol. 3, No. 4, 261–268, 2019.
14. Higgs 4 RFID IC — Alien Technology, [Online], Available: https://https://www.alientechnology .com/products/ic/higgs-4/, Accessed: Aug. 13, 2022.
15. Liao, S. Y., *Microwave Devices and Circuits*, Pearson Education India, 1990.
16. Son, H. W. and C. S. Pyo, "Design of RFID tag antennas using an inductively coupled feed," *Electronics Letters*, Vol. 41, No. 18, 1, 2005.

17. Kuo, S.-K., S.-L. Chen, and C.-T. Lin, "An accurate method for impedance measurement of RFID tag antenna," *Progress In Electromagnetics Research*, Vol. 83, 93–106, 2008.
18. Rishani, N., J.-M. Laheurte, S. Protat, and R. Shubair, "Optimization of the wheeler cap technique for efficiency measurement of RFID antennas matched to complex loads," *Progress In Electromagnetics Research Letters*, Vol. 98, 25–31, 2021.
19. Kamalvand, P., G. K. Pandey, and M. K. Meshram, "A single-sided meandered-dual-antenna structure for UHF RFID tags," *International Journal of Microwave and Wireless Technologies*, Vol. 9, No.7, 1419–1426, 2017.
20. Park, I.-Y. and D. Kim, "Artificial magnetic conductor loaded long-range passive RFID tag antenna mountable on metallic objects," *Electronics Letters*, Vol. 50, No. 5, 335–336, 2014.
21. Dubok, A. and A. B. Smolders, "Miniaturization of robust UHF RFID antennas for use on perishable goods and human bodies," *IEEE Antennas and Wireless Propagation Letters*, Vol. 13, 1321–1324, 2014.
22. Svanda, M. and M. Polivka, "Matching technique for an on-body low-profile coupled-patches UHF RFID tag and for sensor antennas," *IEEE Transactions on Antennas and Propagation*, Vol. 63, No. 5, 2295–2301, 2015.
23. Jaakkola, K., "Small on-metal UHF RFID transponder with long read range," *IEEE Transactions on Antennas and Propagation*, Vol. 64, No. 11, 4859–4867, 2016.
24. Lopez-Soriano, S. and J. Parron, "Design of a small-size, low-profile, and low-cost normal-mode helical antenna for UHF RFID wristbands," *IEEE Antennas and Wireless Propagation Letters*, Vol. 16, 2074–2077, 2017.
25. Michel, A., V. Franchina, P. Nepa, and A. Salvatore, "A UHF RFID tag embeddable in small metal cavities," *IEEE Transactions on Antennas and Propagation*, Vol. 67, No. 2, 1374–1379, 2018.
26. Ooi, S. Y., P. S. Chee, E. H. Lim, Y. H. Lee, and F. L. Bong, "Stacked planar inverted-L antenna with enhanced capacitance for compact tag design," *IEEE Transactions on Antennas and Propagation*, Vol. 70, No. 3, 1816–1823, 2021.